Modeling internal solitary waves on the Australian North West Shelf

Roger Grimshaw[1)], Efim Pelinovsky[2)], Yury Stepanyants[2, 3)], Tatiana Talipova[2)]

[1)]Department of Mathematical Sciences, Loughborough University, UK

[2)]Laboratory of Hydrophysics, Institute of Applied Physics, Nizhny Novgorod, Russia

[3)]Reactor Operations, ANSTO, Lucas Heights, Menai, NSW, 2234, Australia

30 May 2005

Abstract:

The transformation of the nonlinear internal tide and the consequent development of internal solitary waves on the Australian North West Shelf is studied numerically in the framework of the generalized rotation-modified Korteweg–de Vries equation. This model contains both nonlinearity (quadratic and cubic), the Coriolis effect, depth variation and horizontal variability of the density stratification. The simulation results demonstrate that a wide variety of nonlinear wave shapes can be explained by the synergetic action of nonlinearity and the variability of the hydrology along the wave path.

1. Introduction

Peter Holloway was a pioneer in the study of internal tides and solitary waves on the Australian North West Shelf (NWS). A wide variety of nonlinear waves of solitary and bore-like shapes were observed during the two decades of his most productive work in this region [Holloway, 1983, 1984, 1985, 1987, 1988, 1992]. These studies demonstrated the important role of nonlinearity in the formation of the internal wave field. From Holloway's numerous observations, we can conclude that a typical scenario for the evolution of the quasi-sinusoidal semi-diurnal internal tide is analogous to that of an evolving simple (Riemann) wave, with incipient shock wave formation at the leading or trailing edges, and the subsequent disintegration into packets of short-period solitary waves. Some typical examples of such observations, including table-like solitons and groups of isolated short-scale solitons, are demonstrated in Fig. 1. Nonlinear internal waves on the NWS have also been observed from satellites [Baines, 1981; GOA, 2004] and Fig. 2 shows isolated wave with quasi-planar fronts, and groups of short-scale waves with curvilinear fronts.

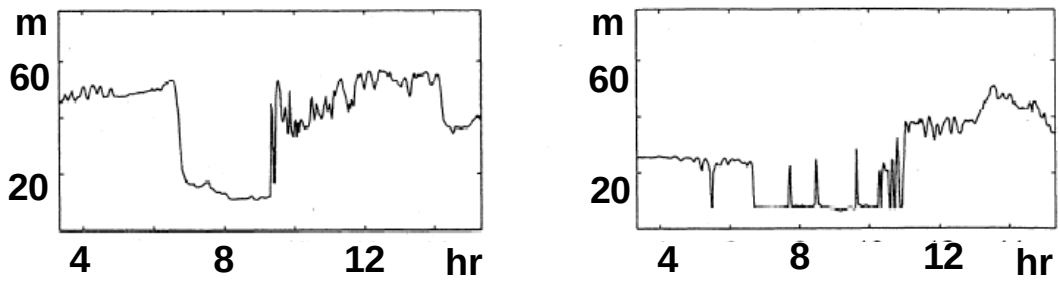

Fig. 1. Displacement of the 25°C isotherm observed on 2 April (left) and 25 March (right) 1992 (from [Holloway et al, 1999]).

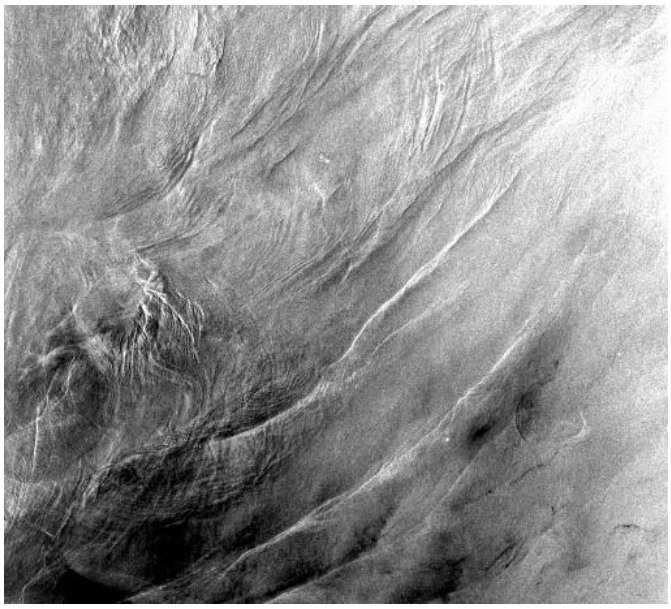

Fig. 2. Satellite image of internal waves on the Australian North West Shelf [GOA, 2004].

There have been several numerical and theoretical modeling studies of internal tides and solitary waves on the NWS. For instance, the Princeton Ocean Model, based on the nonlinear primitive equations, shows a high degree of spatial variability in the amplitude and phase of internal wave currents and vertical displacements [Craig, 1988; Holloway, 1996; Holloway and Barnes, 1998]. On the other hand, weakly nonlinear and weakly dispersive models based on generalizations of the Korteweg–de Vries (KdV) equation also demonstrate the appearance of intense short-scale solitons from the internal tide on the NWS [Smyth & Holloway, 1988; Holloway et al, 1997, 1999, 2001; Grimshaw et al, 2004]. Together these numerical and theoretical modeling studies demonstrate the important role of each of nonlinearity, dispersion, the Earth's rotation, the bottom slope and the horizontal variability of density stratification and the background current. These combined effects lead to the existence of a wide variety of nonlinear waves on the NWS, including forward and backward shocks, solitary waves of positive and negative polarities, table-like (or thick) solitons.

In a recent paper Grimshaw et al (2004) used a generalized Korteweg–de Vries equation to simulate the propagation of an internal solitary wave in a real oceanic environment; they studied the present NWS, and also the Malin Shelf off the west coast of Scotland, and the Arctic Shelf in the Laptev Sea. In this present paper we complement and extend that study by focusing solely on the NWS, and including the effects of the Earth's rotation, which was not considered by Grimshaw et al (2004). As in Grimshaw et al (2004) the main goal is to determine the breakdown of an initial soliton into a complex waveform, taking into account the spatial variability of hydrology and the depth variation in the coastal zone. The basic generalized KdV equation is briefly described in section 2. The coefficients of the model are calculated using the hydrological data on the NWS obtained by Holloway et al (1997, 1999); they are presented in section 3. Our results of numerical simulation of the solitary wave dynamics on the NWS are presented in section 4.

2. Generalized Korteweg–de Vries equation

Until the 1990s the classical KdV equation was a popular model to describe the properties of the observed internal solitary waves, see, for instance, the review papers by Grimshaw (1983) and Ostrovsky & Stepanyants (1989). Then, with increasing and more detailed internal wave observations, it was found that several further factors should be included in the model. First of all, the variable depth along the wave path leads to wave amplitude variation, and even to the possible changing of the soliton polarity; this effect has also been recently studied in the South China Sea [Liu et al, 1998; Cai et al, 2002; Zhao et al, 2003]. Second, the horizontal variability of the density and background current field is important, particularly for the NWS situated at ~20°S [Holloway et al, 1997]. Third is the cubic nonlinear effects which are often comparable with quadratic nonlinearity in tropical conditions [Holloway et al, 1999]. Fourth there is the Coriolis effect due to the Earth's rotation which influences the number and

amplitudes of the solitons generated from the internal tide [Gerkema, 1996]. All these factors are included in the theoretical model consisting of the generalized KdV equation [Holloway et al, 1999, 2001, Grimshaw et al, 2004]. The basic equation of this model is

$$\frac{\partial \varsigma}{\partial x} + \left(\frac{\alpha Q}{c^2}\varsigma + \frac{\alpha_1 Q^2}{c^2}\varsigma^2 \right) \frac{\partial \varsigma}{\partial s} + \frac{\beta}{c^4}\frac{\partial^3 \varsigma}{\partial s^3} = \frac{f^2}{2c}\int_{-\infty}^{s} \varsigma ds \,, \qquad (1)$$

where $\zeta(x,s)$ is the wave amplitude function determining the spatial evolution of the vertical displacement on the isopycnal surface $\xi(x, z, t)$

$$\xi(x,z,t) = \Phi(z,x)Q(x)\varsigma(x,t) + T(z,x)Q^2(x)\zeta^2(x,t) \; + \; \ldots \qquad (2)$$

to the second order of approximation in the wave amplitude. Here x is distance along the wave path, and s is the "local" time, defined below in Eq. (7). $\Phi(z, x)$ is the modal function of long internal waves in the linear approximation. It is found from the following eigenvalue problem,

$$\frac{\partial^2 \Phi}{\partial z^2} + \frac{N^2(z,x)}{c^2(x)}\Phi = 0 \,, \qquad \Phi(z=0) = 0 \,, \qquad \Phi\big(z = -H(x)\big) = 0 \,, \qquad (3)$$

where $z = 0$ corresponds to the free surface and $z = –H(x)$ to the seafloor. Here the buoyancy frequency is $N(z, x)$ and the water depth is $H(x)$. Note that the modal equation (3) is to be solved in z, and the x-dependence is parametric. For convenience we have utilized the Boussinesq approximation here; also, we have omitted the effects of the background field since there is insufficient data available to justify its inclusion. For a description of the theory

when these simplifications are not made, see the review paper by Grimshaw (2001). The modal function is normalized at its maximum, so that $\Phi(z_m) = 1$, where the maximum is achieved at $z = z_m$. The solution of the eigenvalue problem (3) determines both the modal function and the speed $c(x)$ of long linear internal waves.

The coefficients of Eq. (1) are expressed in terms of integrals containing the modal function:

$$\beta(x) = \frac{c}{2} \frac{\int_{-H}^{0} \Phi^2 dz}{\int_{-H}^{0} (\partial\Phi / \partial z)^2 dz} \ . \tag{4}$$

$$\alpha(x) = \frac{3c}{2} \frac{\int_{-H}^{0} (\partial\Phi / \partial z)^3 dz}{\int_{-H}^{0} (\partial\Phi / \partial z)^2 dz} , \tag{5}$$

$$Q(x) = \sqrt{\frac{(Mc^3)_0}{Mc^3}} , \qquad M(x) = \int_{-H}^{0} (\partial\Phi / \partial z)^2 dz , \tag{6}$$

The term with a subscript "0" is for a value at the point $x = 0$ corresponding to the incident wave. Finally in Eq. (1) f is the Coriolis parameter ($f = 2\Omega \sin\theta$ with Ω being the frequency of the Earth's rotation and θ being the local latitude [Grimshaw et al., 1998]), and s is the "running time" which is determined as

$$s = \int_{0}^{x} \frac{dx}{c} - t. \tag{7}$$

The coefficient of the cubic nonlinear term is

$$\alpha_1(x) = \frac{\int_{-H}^{0} \left\{ 3c \left[3\left(\frac{\partial T}{\partial z}\right) - 2\left(\frac{\partial \Phi}{\partial z}\right)^2 \right] \left(\frac{\partial \Phi}{\partial z}\right)^2 - \frac{\alpha^2}{c}\left(\frac{\partial \Phi}{\partial z}\right)^2 + \alpha \left[5\left(\frac{\partial \Phi}{\partial z}\right)^2 - 4\frac{\partial T}{\partial z} \right] \left(\frac{\partial \Phi}{\partial z}\right) \right\} dz}{\int_{-H}^{0} \left(\frac{\partial \Phi}{\partial z}\right)^2 dz}, \qquad (8)$$

and the nonlinear correction to the mode can be found from the ordinary differential equation

$$\frac{\partial^2 T}{\partial z^2} + \frac{N^2}{c^2} T = -\frac{\alpha}{c^2} \frac{\partial^2 \Phi}{\partial z^2} + \frac{3}{2} \frac{\partial}{\partial z} \left[\left(\frac{\partial \Phi}{\partial z} \right)^2 \right] \qquad (9)$$

with the boundary conditions: $T(-H) = T(0) = 0$ and $T(z_m) = 0$. Note that we use so-called time-like Korteweg–de Vries Eq. (1) in the form where spatial and time variables are interchanged. This form is relevant for the observational data analysis of time series measured at fixed spatial places, while the KdV equation in its standard form is relevant for the initial value problem when the snapshot of the wave profile is available.

Before proceeding further, let us note that strictly speaking, Eq. (1) should also include a term due to frictional effects (see, e.g. [Holloway et al, 1997, 1999]). However, the dissipative decay length has been estimated as typically about 100 wavelengths [Craig, 1991; Holloway, 1997, 1999], or about 100 km for the NWS. Since here we are considering internal solitary wave evolution for distances which are essentially less than this, dissipative effects have been omitted, since we expect that the role of friction will then be less than that of the other effects we have included, such as the nonlinearity and the horizontal variability of the hydrology.

The "initial condition" at $x = 0$ for the generalized KdV Eq. (1) corresponds to the incident wave, $\zeta(x = 0, t)$, which should in general be determined from observations of the vertical displacement, $\xi(x = 0, z, t)$ combined with the use of the truncated series (2). The boundary

conditions (in time) for the generalized KdV equation are periodic, with the dominant period of the internal tide; for the NWS this is the semidiurnal period. Eq. (1) has two integrals which are used to monitor the numerical simulations,

$$I_1 \equiv \int_0^T \varsigma(s,x)ds = \int_0^T \xi(t,x=0)dt = \text{const}\,, \qquad I_2 \equiv \int_0^T \varsigma^2(s,x)ds = \int_0^T \xi^2(t,x=0)dt = \text{const}\,. \qquad (10)$$

Note that the first integral, which can be interpreted as related to mass conservation, is identically zero if the Coriolis parameter $f \neq 0$. The second integral is that for wave action flux conservation.

This model is valid for long internal waves of weak and moderate amplitudes, and one simple criterion for this is the smallness of the nonlinear correction to the linear speed; this criterion is checked in all of our simulations. Recently, Small and Hornby (2005) made some comparisons of simulations obtained within the framework of the extended KdV equation (but without the Coriolis term) and a fully nonlinear model for moderate-amplitude internal waves, and showed that the extended KdV equation "works" quite well to describe nonlinear wave evolution.

3. Hydrology of the Australian North West Shelf

Most of Holloway's observations of the internal tide and solitary waves were made in the area of the NWS shown in Fig. 3. In the deep water (marked by the symbol C13 in the figure), the buoyancy frequency profile has one large maximum at depth 40 m, which corresponds to the existence of a sharp pycnocline (Fig. 4a). In the transition zone from deep to shallow water the pycnocline spreads and at depths less than 250 m, the pycnocline disappears which results

in an almost uniform buoyancy frequency profile in average (Figs. 4b, c). In shallow water the buoyancy frequency profile contains two smooth pycnoclines with the biggest one near the seafloor (Fig. 4d). Such large variations of the density stratification lead to a variety of nonlinear wave shapes (e.g. [Holloway et al., 1997, 1999]).

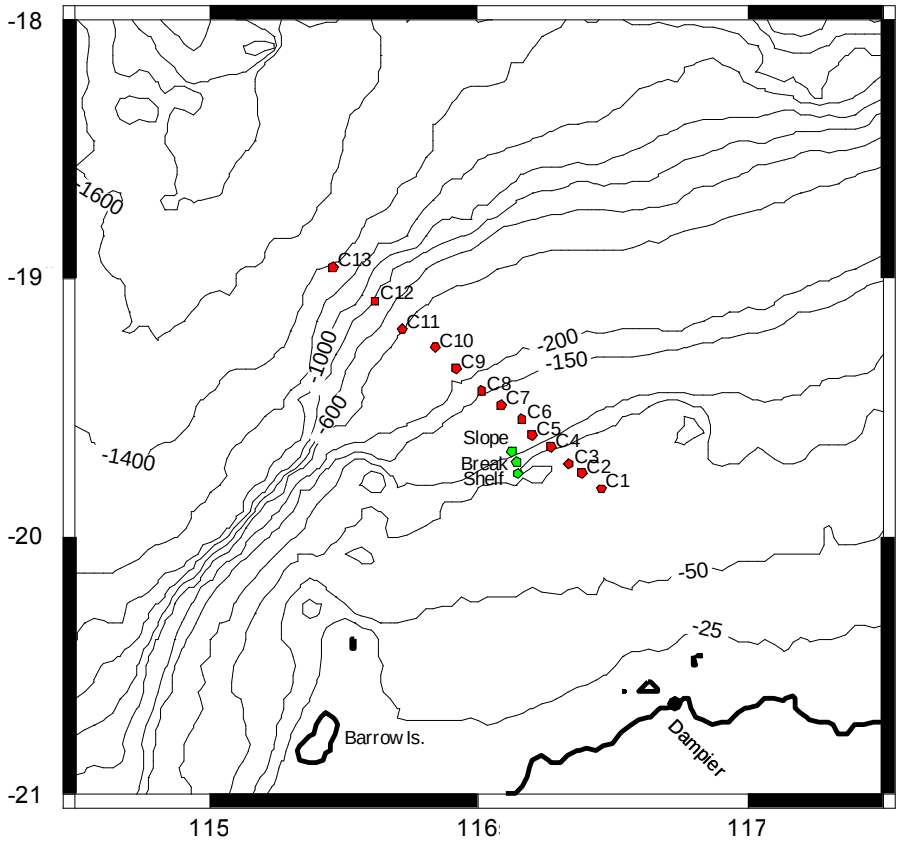

Fig. 3. Map of the region of observations from the Australian North West Shelf showing mooring locations Break and Shelf and temperature-salinity measurement locations C1 to C13 (from [Holloway et al, 1999]).

According to our present theoretical model, such a variety of nonlinear wave shapes may be related to the large variability of the coefficients of the generalized KdV equation through the horizontal variability of the buoyancy frequency profile and through the variable depth. In particular, the nonlinear coefficients (α and α_1) vary significantly, even changing sign, and this induces the complicated dynamics of the nonlinear wave field. The computed coefficients

of the generalized KdV equation are presented in Fig. 5 along the line of CTD stations shown in Fig. 3 (length 100 km, depth is varied from 1400 to 60 m). The linear speed of wave propagation monotonically decreases with depth from 1.4 m/s to 0.3 m/s. The coefficient Q in Eq. (6) describing the linear amplification effect due to the hydrology variability varies from 1 to 4, and therefore even within the linear theory of long waves the wave amplitude may grow up 4 times when the wave approaches the coast.

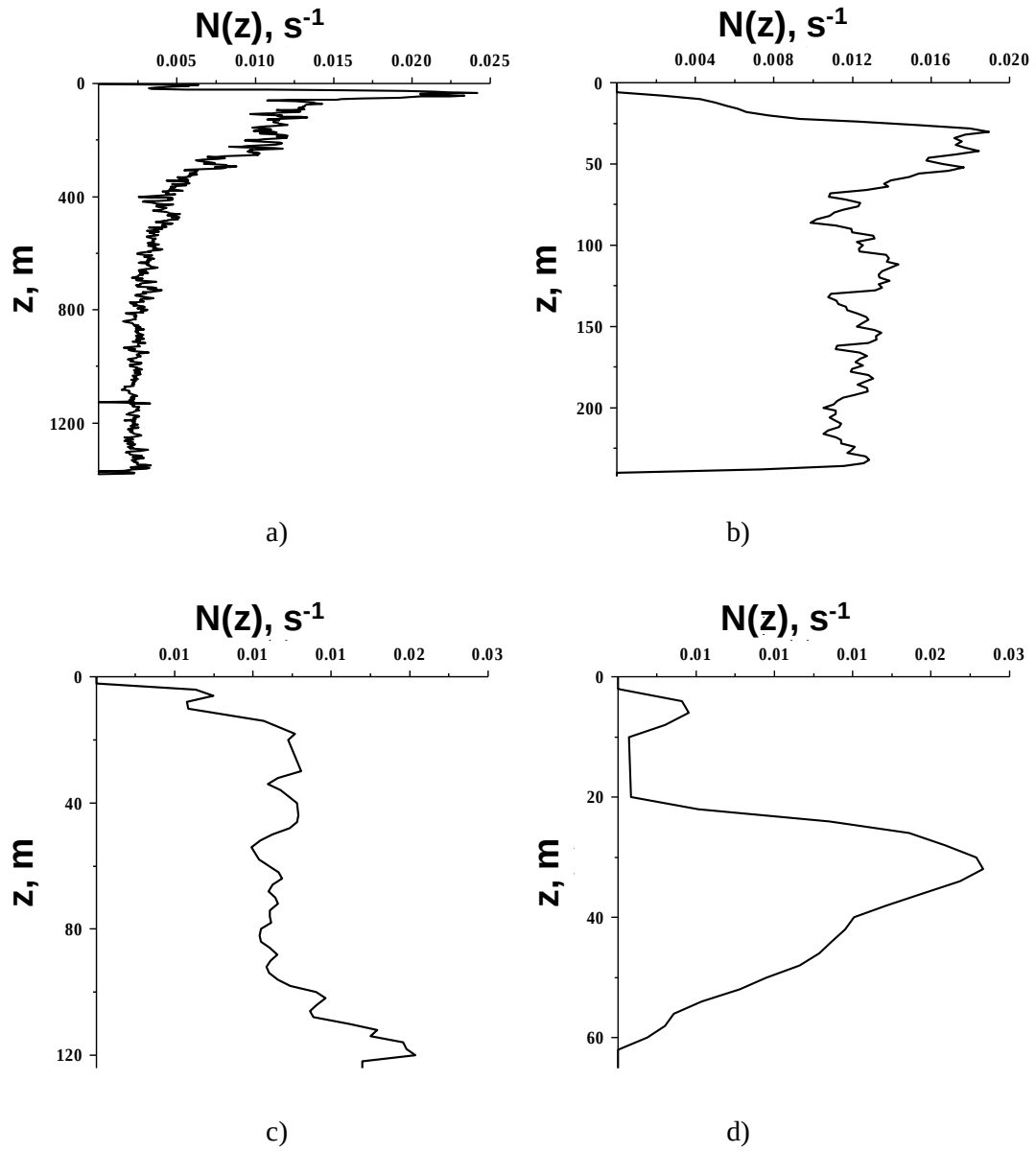

Fig. 4. Buoyancy profiles: (a) at depths 1380 m – 0 km of wave travelling; (b) 240 m – 64.5 km of wave travelling; (c) 120 m – 97.5 km of wave travelling; and (d) 70 m – 122 km of wave travelling.

But in practice, the nonlinear and dispersive effects have a more important effect on the wave amplitude and shape. The dispersion coefficient decreases significantly with depth (through several orders of magnitude), and the role of the nonlinear terms increases. The coefficient of quadratic nonlinearity, α, is negative for deep water, and positive for shallow water passing through a zero value twice. The coefficient of cubic nonlinearity, α_1 being small for deep water is positive for intermediate depth and negative for shallow water. Such a large variability of the coefficients leads to a strong variability of the wave profile, as will be seen in the next section.

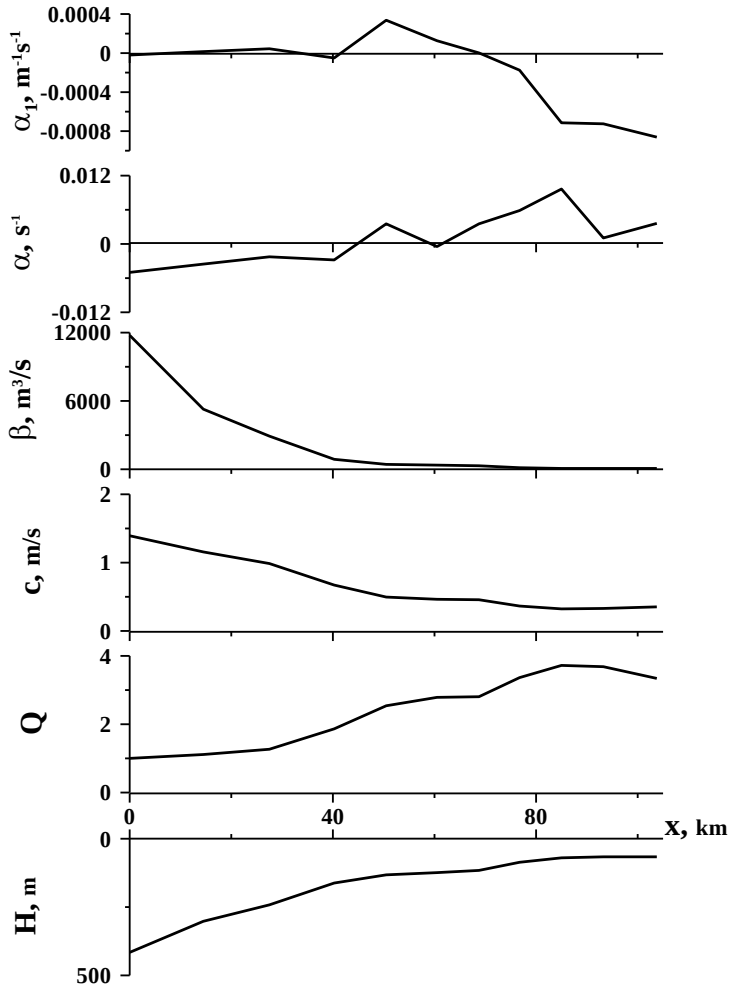

Fig. 5. Variation of the coefficients of the generalized KdV equation for conditions of the NWS.

4. Simulations of wave evolution on the North West Shelf

The numerical model is initialized with the "thick" soliton; that is, the soliton solution of Eq. (1), without the Coriolis term and the magnification term (such an equation is called the extended KdV equation, or Gardner equation) and with constant coefficients,

$$\varsigma(s) = \frac{A}{1 + B\cosh[\gamma(s - s_0)]}, \qquad A = \frac{6\beta\gamma^2}{\alpha c^2}, \qquad \gamma = \sqrt{\frac{\alpha^2 c^2}{6\alpha_1 \beta}(B^2 - 1)}\,. \tag{11}$$

The soliton amplitude is a, not to be confused with the parameter A,

$$a = \frac{A}{1 + B} = \frac{\alpha}{\alpha_1}(B - 1)\,. \tag{12}$$

The whole soliton family can be characterized by two parameters: amplitude, a, and phase, s_0. Equation (1) is then solved in a periodic domain in time (that is, in s) with a period of 12 h corresponding to the semidiurnal tidal cycle (the lower limit in the integral term on the right-hand side of Eq. (1) is now set at the left-hand (rear) boundary); also for convenience of graphic presentation, the initial phase is chosen as s_0 = 6.2 h. The initial wave amplitude is widely varied, but here we present results for the amplitude a = 10 m only. In the following figures the wave displacement is shown at the depth where the maximum of the linear mode is located. The value of $\xi(t, z_m, x) = Q(x)\zeta(t, x)$ is shown at different distances from the deepest point (point C13 in Fig. 3 at depth 1400 m) in the onshore direction. The full wave profile at any depth can be obtained from Eq. (2).

Grimshaw et al (2004) described a set of simulations based on Eq. (1) for the NWS, and also for the Malin Shelf and Arctic Shelf. The simulations we describe here complement and extend those results by including the Coriolis term, and by given some more details of the NWS case; also here we will consider the consequences of omitting the cubic nonlinear term. Thus the first simulation we describe here is for the KdV Eq. (1) when the cubic nonlinear term and the Coriolis effect are both ignored, that is, we set $\alpha_1 = 0$ and $f = 0$ in Eq. (1). In this case the soliton (11) becomes the KdV soliton

$$\zeta(s) = a\,\mathrm{sech}^2\left[\sqrt{\frac{\alpha a}{12\beta}}c(s - s_0)\right]. \tag{13}$$

The wave evolution for this case is displayed in the left panel of Fig. 6. After traveling for 40 km, when the dispersion coefficient has been significantly reduced, the initial depression solitary wave has transformed to an oscillatory wave train (similar to an Airy function). The wave amplitude has increased, but not four times as predicted by the linear long wave theory; this is a consequence of the influence of dispersion on the wave packet. Because the quadratic nonlinear term in shallow water is positive, an elevation solitary wave is formed at a distance of 70 km.

Next we take the Coriolis term into account, but continue to ignore the cubic nonlinear term ($f = 5\cdot10^{-5}$ s^{-1}, $\alpha_1 = 0$); the result is shown in the right panel of Figuire 6; we see that there are no significant qualitative changes in the wave profile (compare with the right panel in Fig. 6). However, the leading wave height (trough-to-crest) is significantly higher (by more than 6 m). A possible reason for this is that in the absence of both dispersion and the Coriolis term, the

maximum amplitude (relative to Q) of a wave is conserved, but the presence of a non-zero Coriolis effect removes this constraint.

The second set of simulations takes account of the cubic nonlinear term, but ignores the Coriolis effect ($f = 0$, $\alpha_1 \neq 0$). The presence of cubic nonlinearity changes the wave shape radically. Compared with the KdV model, the number of waves is less and their amplification is not so high (see the left panel in Fig. 7). Here also one can see the transformation of a depression wave to elevation waves due to the change in sign of the coefficient of quadratic nonlinearity. Further, importantly, the wave amplitudes within the group are not ordered, as was the case when the cubic nonlinearity was ignored. The Coriolis term again influences the wave transformation only weakly (see the right panel in Fig. 7).

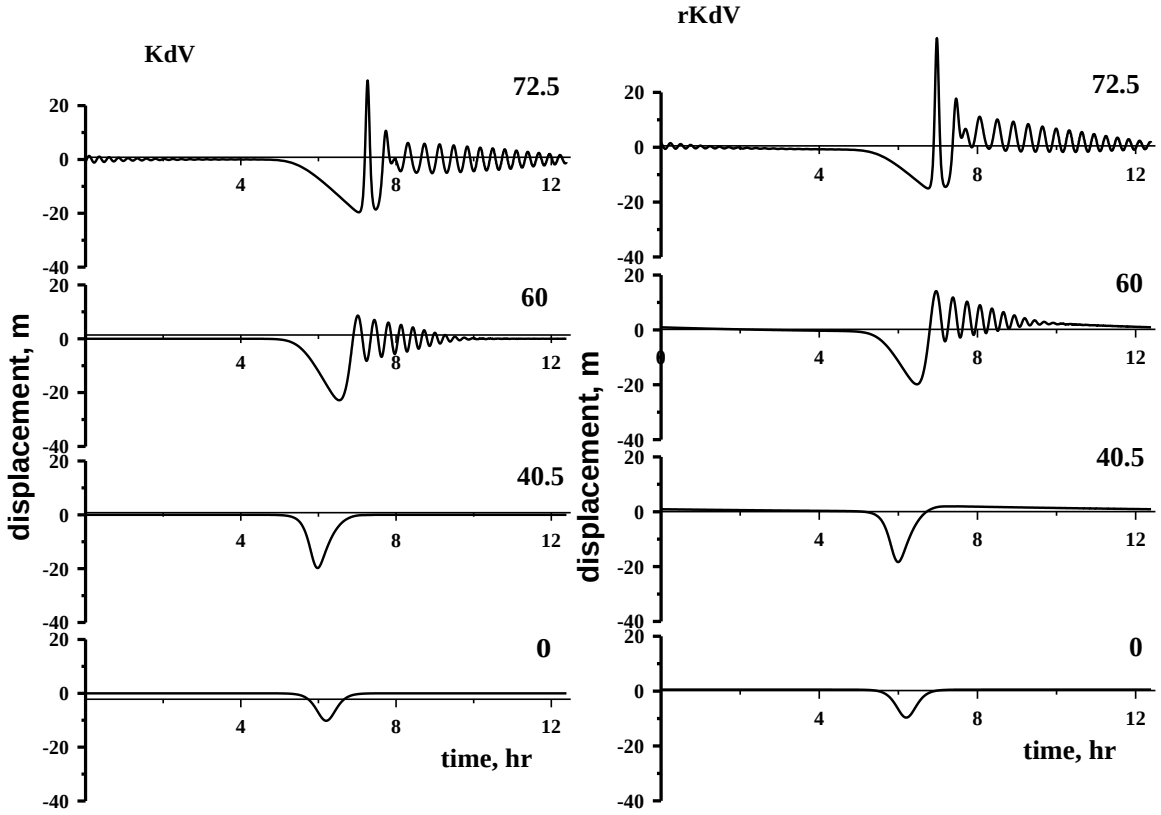

Fig. 6. Wave evolution when cubic nonlinearity is ignored (left/right – without/with the Coriolis term). Numbers indicate distance in km.

The third set of simulations was conducted for a quasi-cnoidal wave of height 10 m in the framework of the full generalized KdV Eq. (1); the results are shown in Fig. 8. Here the initial perturbation was created by the linear superposition of nine solitons sitting on a constant pedestal, chosen so that the total mass of the perturbation was zero in accordance with Eq. (10). Again, one can clearly see the changing of the polarity of the internal waves with distance, due to the change of sign of the coefficient of quadratic nonlinearity. The wave height is increased in shallow water up to four times, and the resulting wave shapes show the complicated character of the wave field.

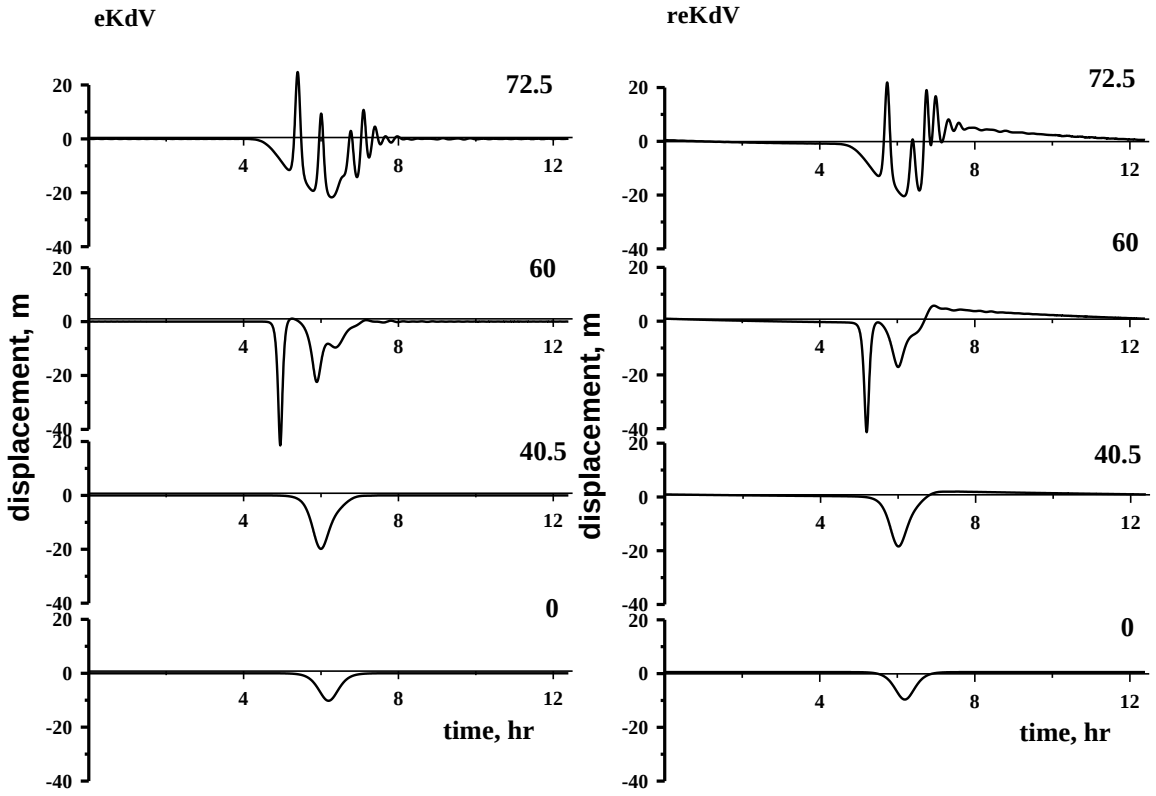

Fig. 7. Wave evolution taking account of cubic nonlinearity (left/right – without/with the Coriolis effect). Numbers indicate distance in km.

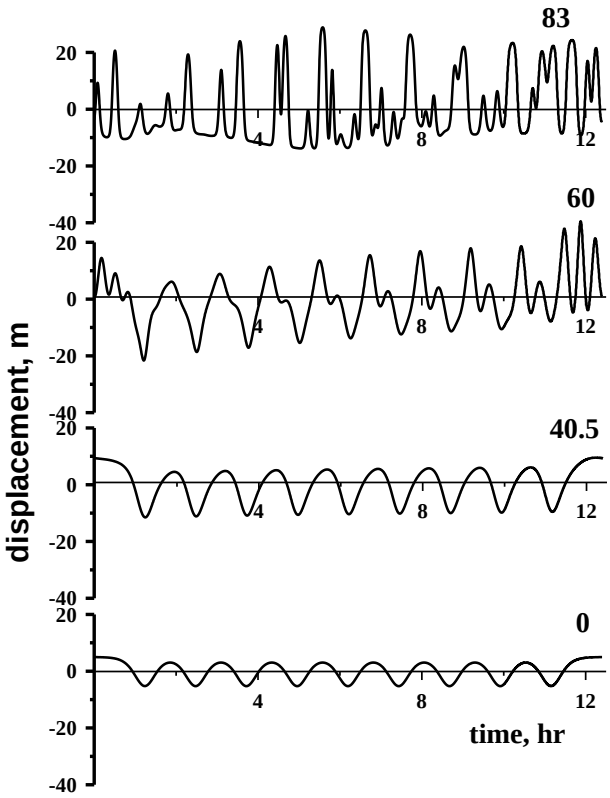

Fig. 8. Periodic wave evolution on the Australian North West Shelf. Numbers indicate distance in km.

There are groups of solitons of positive polarity and different heights, as well as shock-like disturbances. These profiles look quite like those observed in the ocean (see, e.g. right panel in Fig. 1).

5. Conclusion

This paper is dedicated to the memory of Peter Holloway, who stimulated our study of internal waves on the NWS. The wide variety of observed internal solitary wave shapes can be explained theoretically by the synergetic action of cubic nonlinearity and the strong horizontal variability of the bottom topography and the density stratification. From our simulations of the generalized KdV equation (1) presented here, we conclude that, for internal solitary waves with amplitudes typical for the NWS, cubic nonlinearity plays a very

significant role vis-à-vis quadratic nonlinearity. On the other hand the Coriolis effect does not change the wave profiles qualitatively, at least for the time and space scales considered here. We conclude, from the small sample of our numerical simulations presented here, and other analogous simulations not shown here, that the generalized KdV equation (1) can indeed demonstrate the kind of variability in the internal wave profiles that has been observed on the NWS.

Acknowledgement

This study is supported by grants from ONR (RG), INTAS (03-51-3728 and 03-51-4286) and RFBR (03-05-64978 and 04-05-3900) (EP, TT).

References

Baines, P.G. Satellite observations of internal waves on the Australian North West Shelf. *Aust. J. Mar. Freshwater Research*, 1981, vol. 32, 457–463.

Cai, S., Long, X., and Gan, Z. A numerical study of the generation and propagation of internal solitary waves in the Luzon Strait. *Oceanologica Acta*, 2002, vol. 25, 51–60.

Craig, P.D. A numerical model study of internal tides on the Australian North West Shelf. *J. Marine Research*, 1988, vol. 46, 59–76.

Craig, P.D. Incorporation of damping into internal wave models. *Continental Shelf Research*, 1991, vol. 11, No. 6, 563–577.

Gerkema T. A unified model for the generation and fission of internal tides in a rotating ocean. *J. Marine Res.*, 1996, v. 54, 421–450.

Global Ocean Associates. *An atlas of oceanic internal solitary waves*, 2004, 506–518. http://www.internalwaveatlas.com

Grimshaw, R. Solitary waves in slowly varying environments: long nonlinear waves. In: *Nonlinear Waves* (Ed. L.Debnath). Cambridge Univ. Press. 1983, 44–67.

Grimshaw, R. Internal solitary waves. In: *Environmental Stratified Flows* (Ed. R. Grimshaw) , Kluwer, Boston, (2001), Chapter 1, 1-29.

Grimshaw, R.H.J., Ostrovsky L.A., Shrira V.I., and Stepanyants Yu.A. Long nonlinear surface and internal gravity waves in a rotating ocean. *Surveys in Geophysics*, 1998, vol. 19, n. 4, 289–338.

Grimshaw, R., Pelinovsky, E., Talipova, T. and Kurkin, A. Simulation of the transformation of internal solitary waves on oceanic shelves. *J. Phys. Ocean*., 2004, vol. 34 , 2774–2779.

Holloway, P.E. Internal tides on the Australian North-West Shelf: a preliminary investigation. *J. Phys. Oceanog.*, 1983, vol. 13, 1357–1370.

Holloway, P.E. On the semidiurnal internal tide at a shelf break region on the Australian North West Shelf. *J. Physical Oceanography*, 1984, vol. 14, 1787–1799.

Holloway, P.E. A comparison of semidiurnal internal tides from different bathymetric locations on the Australian North West Shelf. *J. Physical Oceanography*, 1985, vol. 15, 240–251.

Holloway, P.E. Internal hydraulic jumps and solitons at a shelf break region on the Australian North West Shelf. *J. Geophys. Research*, 1987, v. 92, No. C5, 5405–5416.

Holloway, P.E. Climatology of internal tides at a shelf-break region on the Australian North West Shelf. *Aust. J. Mar. Freshwater Research*, 1988, vol. 39, 1–18.

Holloway, P.E. Observations of shock and undular bore formation in internal waves at a shelf break. *Breaking Waves* (Eds. M.Banner and R.Grimshaw). Springer, Berlin, 1992, 367–373.

Holloway, P.E. Observations of internal tide propagation on the Australian North West Shelf. *J. Physical Oceanography*, 1994, vol. 14, n. 8, 1706–1716.

Holloway, P.E. A numerical model of internal tides with application to the Australian North West Shelf. *J. Physical Oceanography*, 1996, vol. 26, 21–37.

Holloway, P.E., Pelinovsky, E., Talipova, T., and Barnes, B. A nonlinear model of internal tide transformation on the Australian North West Shelf. *J. Physical Oceanography*, 1997, vol. 27, n. 6, 871–896.

Holloway, P.E., and Barnes, B. A numerical investigation into the bottom boundary layer flow and vertical structure of internal waves on a continental slope. *Continental Shelf Research*, 1998, vol. 18, 31–65.

Holloway, P, Pelinovsky, E., and Talipova, T. A Generalised Korteweg–de Vries model of internal tide transformation in the coastal zone. *J. Geophys. Research*, 1999, vol. 104, No. C8, 18,333–18,350.

Holloway, P., Pelinovsky, E., and Talipova, T. Internal tide transformation and oceanic internal solitary waves. Chapter 2 in the book: *Environmental Stratified Flows* (Ed. R. Grimshaw). Kluwer Acad. Publ., Boston–Dordrecht–London, 2001, 29–60.

Liu, A. K., Chang, S.Y., Hsu, M-K., and Liang, N.K. Evolution of nonlinear internal waves in East and South China Seas, *J. Geophys. Res.*,1998, vol. 103, 7995– 8008.

Ostrovsky, L.A., and Stepanyants, Yu.A. Do internal soliton exist in the ocean? *Rev. Geophys*., 1989, vol. 27,293–27,310.

Small, R.J., and Hornby, R.P. A comparison of weakly and fully nonlinear models of the shoaling of a solitary internal wave. *Ocean Modelling*, 2005, vol. 8, 395–416.

Smyth, N.F., and Holloway, P.E. Hydraulic jump and undular bore formation on a shelf break. *J. Physical Oceanography*, 1988, vol. 18, No. 7, 947–962.

Zhao, Z., Klemas, V.V., Zheng, Q., and Yan, X-H. Satellite observation of internal solitary waves converting polarity. *Geoph. Res. Lett*., 2003, vol. 30, n. 19, 1988, doi:10.1029/2003GL018286.